ORIGINAL ARTICLE

Micro-milling force modeling with tool wear and runout effect by spatial analytic geometry

Guochao Li[1,2] · Si Li[2] · Kunpeng Zhu[2]

Abstract

One of the major limitations of micro-milling applications in industries is its fast tool wear, which leads to low machining precision and efficiency. An accurate force model is fundamental for optimization micro-milling processes and minimize the tool wear. However, a generic model with tool runout and wear effect has not yet been established, which limits its practical application under varied working conditions. In this paper, a new idea is introduced by applying the spatial analytic geometry (SAG) method, under this framework the micro-milling force model is established based on the analysis of the geometrical relationship among the cutting edge positions, pre-processed workpiece morphology, and cutting force directions considering tool runout and wear effect. In this model, the tool runout is identified exclusively by only one parameter, namely the distance away from the center that perpendicular to the feed direction, so that it could be calibrated conveniently by calculating the ratio of resultant forces corresponding to different cutting edges. The tool wear–induced force is then modeled as increment of force coefficients to the original model. Therefore, the new force model with considering tool wear has the same form as the fresh tool. Finally, the accuracy and efficiency of the model are validated by experiments under varied working conditions.

Keywords Micro-milling force · Tool runout · Tool wear · Spatial analytic geometry

Nomenclature

SA	Spatial analytic geometry
UCT	Uncut chip thickness
$X_w Y_w Z_w$-O_w	Workpiece coordinates
$X_T Y_T Z_T$-O_T	Tool coordinates
$X_S Y_S Z_S$-O_S	Spindle coordinates

dF_r, F_r	Radial force
dF_t, F_t	Tangential force
φ	Rotation angle of the tool
K_{tc}, K_{rc}	Coefficients of tangential and radial force
dh_j	UCT of the discrete element
db	Length of the discrete element along the tool edge
Nj	Amount of the discrete element
r_1, r_2	Rotating radius around the Z_S-axis for the two edges
r_{out}	Tool runout
x_{out}, y_{out}	Tool axis position parameters
θ_{out}	Angle between Y_S-axis and linkage of tool edge and center
r_t	Tool radius
f_t	Feed per tooth
r_{ts1}, r_{ts2}	Rotation radiuses of the two edges
K_{tc}^{wear}, K_{rc}^{wear}	Coefficients of tangential and radial force considering tool wear
P	Tool lead
N	Number of edges

✉ Guochao Li
liguochaolaile@126.com

✉ Kunpeng Zhu
zhukp@iamt.ac.cn

Si Li
sili@iamt.ac.cn

1 School of Mechanical Engineering, Jiangsu University of Science and Technology, Zhenjiang 212003, China

2 Institute of Advanced Manufacturing Technology Hefei Institutes of Physical Science, Chinese Academy of Science, Huihong Building, Changwu Middle Road 801, Changzhou 213164, Jiangsu, China

1 Introduction

Micro-milling has been widely used in the aerospace, medical, electronic, optics, and other industries, due to its good performance in machining micro-components with diverse materials and free-form surfaces [1]. In a sense, micro-machining process can be considered a scale down version of conventional machining process. However, as the cutting tool radius (less than 1 mm) [2], cutting edge radius (0.1~1 μm), the feed rate (1~10 μm), and the workpiece material grain size (1~10 μm) have the similar scale, micro-milling has different cutting mechanisms, such as minimum chip thickness [3], non-ignorable tool runout, and rapid tool wear. All these lead to problems, such as poor surface quality, low efficiency, and high costs. Modeling and analyzing the force acting on the micro-milling tool is an efficient way to reveal and solve these mechanisms and problems.

Currently, the micro-milling force is mainly studied by analytical [4], experiential [5, 6], numerical [7, 8], and mechanical methods[9–11]. Among them, mechanical method is most studied due to its high accuracy and physical traceability [12]. Its fundamental assumption is that the force is proportional to the uncut chip thickness (UCT), so that its main work is to identify the proportion coefficients and UCT for a milling process. While in micro-milling, tool runout effect should be critically assessed, which is significant on cutting force due to ultra-high spindle speed [13, 14]. In the meantime, the tool wear imposes direct impact on the milling force, including the shearing, plowing, and friction forces, and eventually decreases the accuracy of the established model [15, 16]. Therefore, tool runout and wear effects need to be investigated and included for a precise micro-milling force model.

The micro-milling force model with considering runout is mainly based on the modification of UCT by substituting the tool runout parameters into the cutting edge trajectories [17–20]. For example, Li, et al. [18] firstly computed the UCT by intersecting the normal line of the current cutting edge formed rotary surface with the preceding formed rotary surface, which was formed by each cutting edge undergoing general spatial motion with cutter runout. Then, the UCT was substituted into the model to improve its accuracy. Compared with the force model construction, the calibration of runout parameters for the micro-milling processes is more difficult. By now, cyclic iterative method and direct measurement method are mainly employed. The basic idea of the iterative method is that the runout parameters are firstly used to establish the force model and then calibrated by forces measured from experiments. The calibration processes loops until the minimum difference between the predicted and experimental results is obtained. Ko and Li [21–23] calibrated the cutting force coefficients and runout parameters by synchronizing the simulation and experimental forces in one tool revolution. Wan et al. [24] established a target equation that was the

subtraction of simulation and experimental forces. The equation was solved by the Nelder-Mead simplex method and the runout parameters were then obtained. Zhang et al. [25] carried out a thin plate milling test to make sure that only one edge was involved in cutting processes at any instant. The runout parameter was calculated by comparing the theoretical and experimental contact time between the edge and workpiece. Similarly, Guo et al. [26] provided a rapid mathematical method for the determination of cutter runout parameters in flat-end milling. Differently, Jing et al. [13] reported a direct measurement method by using CCD cameras. The runout parameters were calculated by measuring the tool handle and edge turning radius with geometrical methods. Zhang et al. [27] obtained the tool runout length and tool runout angle by solving some equations related to the cutter parameters, which was based on the displacement measurement. Besides, Attanasio et al. [28] deduced tool run-out from the actual tool diameter, the channel width, and the cutting edge's phase, which is estimated by analyzing the cutting force signal with a high sampling rate.

As discussed above, the cyclic iterative method that used to calibrate the runout parameters is time consuming, and it has an underlying assumption that the tool is perfectly manufactured to ensure its tooth spacing angle, which is not conformed in reality. Besides, the direct measurement method is hard for micro-milling. Therefore, a new idea is proposed in this paper to identify tool runout exclusively by only one parameter, which could be calibrated conveniently by calculating the ratio of resultant forces corresponding to different cutting edges and enhance the practical applications of the model.

As another significant factor, tool wear has little been introduced in force modeling. Most studies have focused on tool wear phenomena or its experimental analysis with force variations only [15, 29–32]. Bao et al. [33] treated the increased force caused by tool wear as wear coefficients in the force model. The wear coefficients were computed by genetic algorithm. Based on FEM and experiments, Oliaei et al. [34] analyzed the impact of tool wear on the force coefficients in circular pocket micro-milling of stainless steel. They found that the cutting force was related to tool wear forms and that flank wear was dominate for milling. Lu et al. [35] firstly obtained the tool flank wear by FEM method and then established the micro-milling force model of nickel-based superalloy with considering tool wear. Thanongsak et al. [36] built the tool wear force model of Ti-6Al-4V in DEFORM software. Jaffery et al. [37] analyzed flank wear progression during micro-machining operation, which showed that when machining with undeformed chip thickness above edge radius, the feed rate remains the most significant parameter affecting tool wear. Although many force models with considering tool wear had been reported, a uniform model for micro-milling is still absent, which has impeded the development of micro-milling technology.

In this study, a new idea is introduced based on the spatial analytic geometry (SAG) method. Different from previous studies, the tool runout parameter is conveniently calibrated by calculating the ratio of resultant forces corresponding to different cutting edges, and the force model with considering tool wear is expressed as a uniform expression.

2 Modeling of micro-milling force with tool runout and wear effect based on the SAG method

2.1 Spatial geometric and force model for micro-milling

The flat micro-end mill with two edges for slot milling is discussed in the study. The main coordinates are displayed in Fig. 1. The workpiece coordinates are denoted as $X_w Y_w Z_w$-O_w, where the X_w-axis is along with the feed direction and the Z_w-axis coincides with the tool axis (Fig. 1(a)). The tool coordinates are denoted as $X_T Y_T Z_T$-O_T, where the Y_T-axis is located in the tool end face and cross the cutting edge, and the Z_T-axis coincides with the tool axis (Fig. 1(b)). Point Q is located on the edge. The edge that intersects with the Y_T-axis is denoted as Edge_1 and the other is Edge_2. The spindle coordinates are denoted as $X_S Y_S Z_S$-O_S, where the Z_S-axis coincides with the spindle axis, the X_S-axis and Y_S-axis are parallel to the X_W-axis and Y_W-axis, respectively.

The milling force acting on the element of tool edge is defined in four directions on the cross-section plane, as presented in Fig.1(c). The radial force dF_r points to the workpiece, tangential force dF_t is normal to dF_r and points to the edge-motion direction, dF_x is along with X_W-axis and points to its positive direction, and dF_y is along with Y_W-axis and points to its positive direction. Their relationships can be written as:

$$\begin{cases} dF_x = dF_r\sin(\phi) + dF_t\cos(\phi) \\ dF_y = dF_r\cos(\phi) - dF_t\sin(\phi) \end{cases} \quad (1)$$

where φ is rotation angle of the tool.

The milling force model is established with four hypotheses: (1) the plow force is neglected because the workpiece material (such as AISI4340) is hard to spring back during the cutting process [38]; (2) the force coefficient stay constant [21]; (3) tool runout is mainly in radial direction [24]; (4) relative to the radial and tangential directions, the force along the tool axis is little enough to be neglected. Thus, according to that the instantaneous cutting force is in proportion to the UCT, the instantaneous milling forces acting on the tool can be expressed as [39, 38]:

$$\begin{cases} F_t = \sum_{j=1}^{Nj} dF_{tj} = \sum_{j=1}^{Nj} K_{tc} dh_j db \\ F_r = \sum_{j=1}^{Nj} dF_{rj} = \sum_{j=1}^{Nj} K_{rc} dh_j db \end{cases} \quad (2)$$

where, F_t and F_r are tangential and radial force of the tool, dF_{tj} and dF_{rj} are tangential and radial force acting on the tool edge discrete element, K_{tc} and K_{rc} are coefficients of tangential and radial force, dh_j is UCT of the discrete element, db is the length of the discrete element along the tool edge, j is the sequence number of the discrete element of cutting edge along the cutting tool axis, and Nj is the amount of the discrete element. Among these parameters, db is assigned manually before modeling, while dh_j, Nj, K_{tc}, and K_{rc} need to be calculated or calibrated by using analytical or experimental method based on the process parameters and tool geometries.

The fundamental definition of dh_j in the jth discrete tool section plane is provided in Fig. 2. Points p_1 and p_2 are located on the tool axis and the Edge_1 respectively. Point p_3 is the intersection of line $p_1 p_2$ and trajectory of Edge_2. Point p_4 is
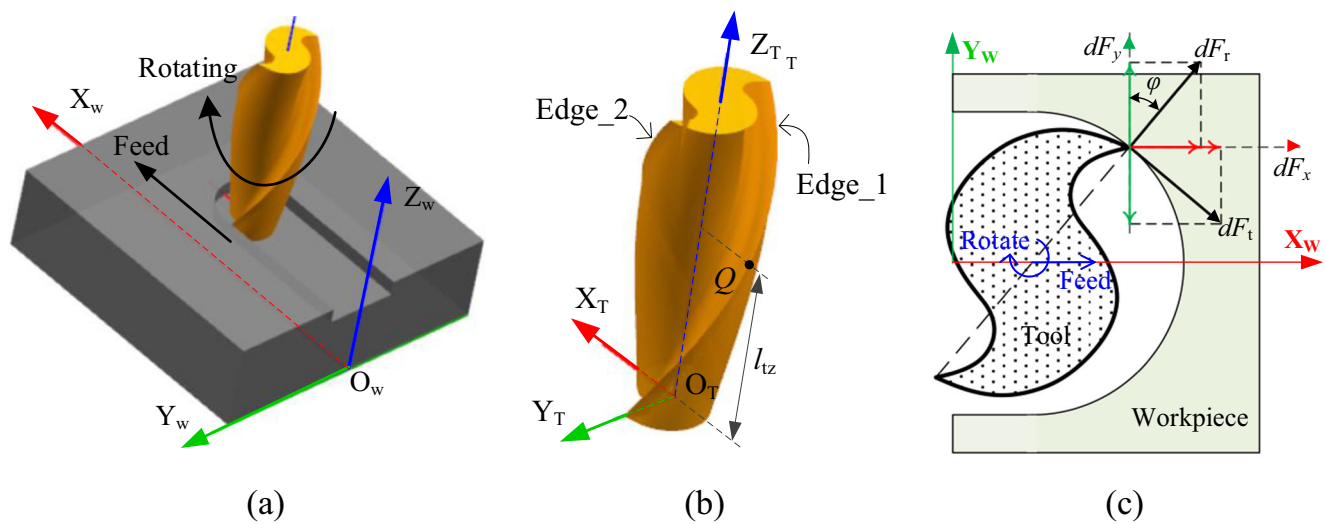

Fig. 1 Coordinates and milling forces of milling process. **a** Workpiece coordinates. **b** Tool coordinates and cutting edge definition. **c** Milling force on the tool cross-section
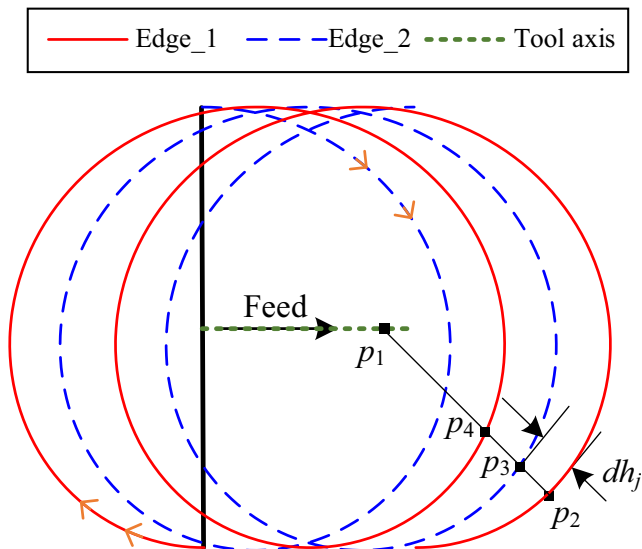
Fig. 2 Fundamental definition of dh_j ($r_t = 0.25$ mm, $f_t = 0.006$ mm)

the intersection of line p_1p_2 and the previous trajectory of Edge_1. Suppose that Edge_1 is involved in cutting process after Edge_2, the dh_j can be deduced as:

$$dh_j = d_{p1p3} - d_{p1p3} = r_t - d_{p1p3} \quad (3)$$

where, d_{p1p2} is the distance between point p_1 and p_2, and d_{p1p3} is the distance between point p_1 and p_3.

Unlike that of the traditional milling process, the micro-milling forces are significantly affected by the tool runout and tool wear. The calculation of h_j, Nj, K_{tc}, and K_{rc} with considering tool runout and wear effect is necessary for the modeling of micro-milling force. The following sections will discuss the influence of tool runout and tool wear on h_j, Nj, K_{tc}, and K_{rc}.

2.2 Definition and identification of tool runout with the SAG method

Essentially, the tool runout is the maximum difference of rotating radiuses of different cutting edges. Take Fig. 3(a) for an example, when the tool with two edges locates on the practice position, the rotating radius around the Z_S-axis for one of the edges is r_1 and for the other edge is r_2, the tool runout can be then evaluated as $r_{out} = r_2 - r_1$, where r_2 and r_1 are decided by three parameters, namely the tool axis position parameters (x_{out} and y_{out}) and the angle (θ_{out}) between Y_S-axis and linkage of tool edge and center.

According to the SAG theory, the values of r_1 and r_2 will remain unchanged when the tool rotates around the Z_S-axis. Take Fig. 3 for an example, the tool presented in Fig.3(a) rotates around the Z_S-axis, through the state shown in Fig.3 (b) and (c), there exist a position that the linkage of the two tool edges is parallel to the Y_S-axis (i.e., $\theta_{out} = 0$), as shown in

Fig. 3(d). Therefore, the runout can be identified exclusively by two parameters x_{out} and y_{out}.

Then, according to Fig. 3(d), the runout can be expressed as:

$$r_{out}(x_{out}, y_{out}) = r_2 - r_1 = \sqrt{x_{out}^2 + (r_t + y_{out})^2} - \sqrt{x_{out}^2 + (r_t - y_{out})^2} \quad (4)$$

where r_t is the tool radius.

According to Eq. (4), the values of r_{out} with various x_{out} and y_{out} are presented in Fig. 4. It showed that the values of r_{out} increased distinctly with y_{out} when x_{out} is constant, while the values of r_{out} almost unchanged with the increasing of x_{out} when y_{out} is constant. Thus, it was reasonably believed that y_{out} has much more effect on r_{out} than x_{out}. So, although runout is used to be defined by four parameters in Cartesian coordinates or two parameters in polar coordinates [14, 17–20], it is reasonable to neglect x_{out} and only to calculate y_{out} to identify the runout, which will improve the efficiency of the calibration process of runout parameter with little accuracy loss. Thus, considering that x_{out} has little effect on r_{out}, substituting $x_{out} = 0$ into Eq.(4), it can conclude that $r_{out} \approx 2 \cdot y_{out}$. Therefore, the tool runout is identified by y_{out} instead of r_{out} in the following sections.

The next is to calibrate the runout parameter. According to Eq. (2), the instantaneous resultant forces of the cutting tool can be induced as:

$$\begin{cases} F_t = \sum_{j=1}^{Nj} k_{tc} h_j db_j \\ F_r = \sum_{j=1}^{Nj} k_{rc} h_j db_j \end{cases} \Rightarrow F_{resultant} = \sqrt{F_t^2 + F_r^2} = \sqrt{(k_{tc}^2 + k_{rc}^2) \sum_{j=1}^{Nj} h_j^2 db_j^2}$$

$$(5)$$

where j and Nj are the numerical order and number of the edge discrete unit.

Considering that the tool position along the spindle axis is consistent and that db is assigned manually before modeling, the length of every discrete element along the two tool edges are equal, namely, $db_j^{edge1} = db_j^{edge2}$. Thus, the ratio between the resultant forces of the two edges can be written as:

$$\frac{F_{resultant}^{edge1}}{F_{resultant}^{edge2}} = \frac{\sqrt{(k_{tc}^2 + k_{rc}^2) \sum_{j=1}^{Nj} \left(h_j^{edge1}\right)^2 \left(db_j^{edge1}\right)^2}}{\sqrt{\sqrt{(k_{tc}^2 + k_{rc}^2) \sum_{j=1}^{Nj} \left(h_j^{edge2}\right)^2 \left(db_j^{edge2}\right)^2}}}$$

$$= \frac{\sqrt{\sum_{j=1}^{Nj} \left(h_j^{edge1}\right)^2}}{\sqrt{\sum_{j=1}^{Nj} \left(h_j^{edge2}\right)^2}} \quad (6)$$
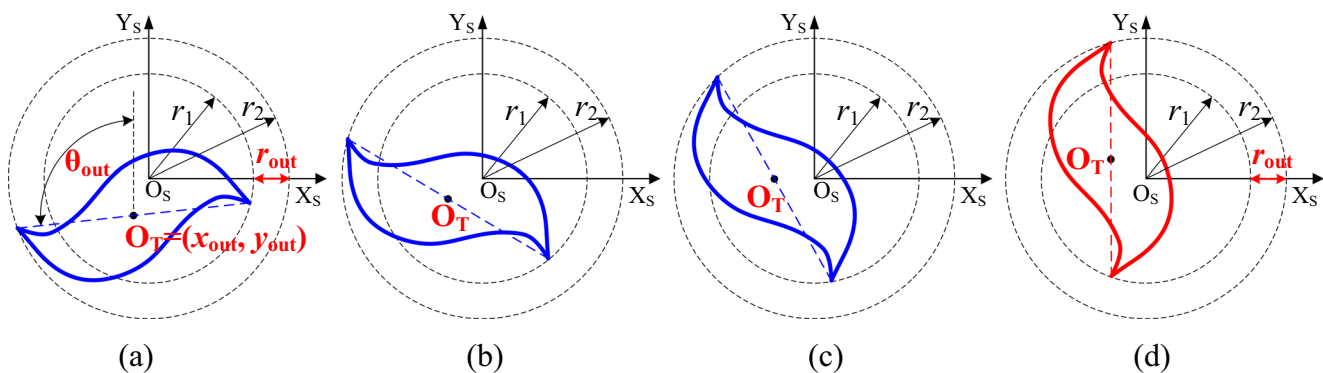
Fig. 3 Runout definition. **a** Practical tool position. **b** The tool rotating around the O_S-axis. **c** The tool rotating around the O_S-axis. **d** The tool rotates to the calculation position, namely $\theta_{out} = 0$

According to Eq.(5), the instantaneous resultant force only depends on the sum of the uncut chip thickness h_j. Therefore, the ratio between the maximum resultant forces of the two edges can be expressed as:

$$\frac{F_{resultant\_max}^{edge1}}{F_{resultant\_max}^{edge2}} = \frac{h_{max}^{edge1}}{h_{max}^{edge2}} \tag{7}$$

As has been discussed above, the tool moves in the positive direction of the X_w-axis (see Fig.1(a)). If the tool runout is inexistent, the maximum UCT for a cutting edge during one tool revolution should be equal to the value of feed per tooth f_t (see Fig. 2). However, if the tool axis deviates from the Y_s-axis with a value of y_{out}, the rotation radiuses of the two edges will be r_{ts1} and r_{ts2} (where, $r_{ts1} = r_t + y_{out}$ and $r_{ts2} = r_t - y_{out}$). Therefore, as shown in Fig. 5, the maximum UCT for slot milling along the X_W-axis can be calculated as:

$$\begin{aligned} h_{max}^{edge1} &= f_t - 2y_{out} \\ h_{max}^{edge2} &= f_t + 2y_{out} \end{aligned} \tag{8}$$
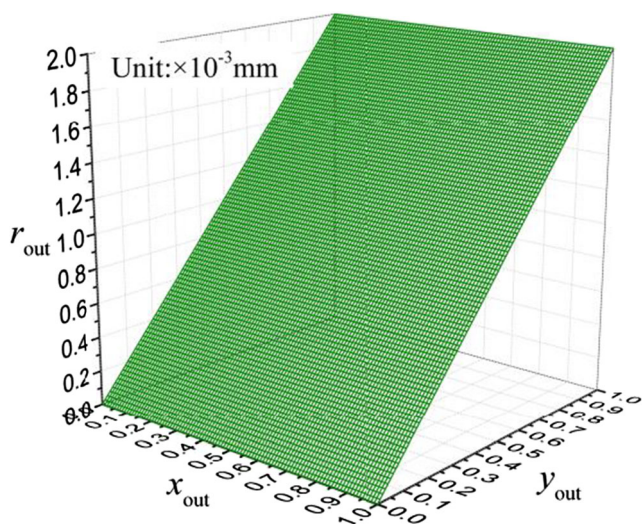

Fig. 4 Values of r_{out} with various x_{out} and y_{out} ($r_t = 0.25$ mm)

Hence, substituting Eq. (8) into Eq. (7), the runout value y_{out} can be deduced as:

$$y_{out} = \frac{(f_z/4)\left(F_{resultant\_max}^{edge1} - F_{resultant\_max}^{edge2}\right)}{F_{resultant\_max}^{edge1} + F_{resultant\_max}^{edge2}} \tag{9}$$

According to Eq. (9), the tool runout could be conveniently identified by the maximum resultant forces of the two cutting edges. It will improve the efficiency and real-time capability of force modeling, which is very important for process control of the micro-milling.

2.3 The micro-milling force with tool runout and wear effect based on the SAG method

The cutting force increases with the tool wear during the micro-milling process. The tool wear for micro-milling is mainly reflected in the rear face, which can be regarded as the little decreasing of the tool radius and the deteriorating of surface of the rear face. The little decreasing of the tool radius will have little effect on the tool runout, which is determined primarily by the difference of rotation radiuses of the two edges, rather than the tool radius. While the deteriorated rear face will remarkably increase the interactional force between the cutting edge and the processed workpiece.

The force model (see Eq.2) contains two kinds of variables, one is the UCT (h_j) and the other is force coefficients (K_{tc} and K_{rc}). Considering that the UCT is mainly affected by tool runout, which is independent on tool wear, it is reasonable to assume that the additional force that affected by tool wear as the addition of force coefficients. Then, according to Eq. (2), the micro-milling force prediction model can be written as:

$$\begin{cases} F_t = \sum_{j=1}^{Nj} dF_{tj} = \sum_{j=1}^{Nj} \left(K_{tc} + K_{tc}^{wear}\right) h_j db \\ F_r = \sum_{j=1}^{Nj} dF_{rj} = \sum_{j=1}^{Nj} \left(K_{rc} + K_{rc}^{wear}\right) h_j db \end{cases} \tag{10}$$

Fig. 5 The maximum UCT for slot milling with tool runout
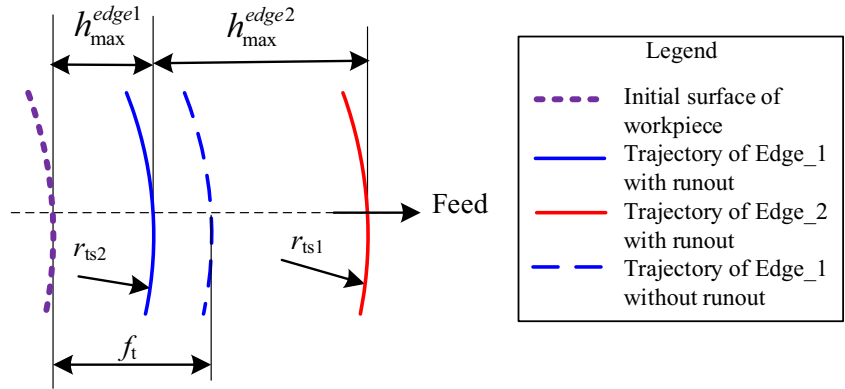
where, K_{tc}^{wear} and K_{rc}^{wear} are coefficients of tangential and radial force considering tool wear.

The UCT could be calculated by Eq. (3) without considering runout effect. While two cases need to be supplemented if tool runout effect is considered. As presented in Fig. 6, case I is that the chip is formed by trajectories that produced by the same cutting edge, and case II is that no chip is formed due to tool runout. Therefore, with considering runout effect, Eq. (3) need to be modified as:

$$dh_j = \begin{cases} \min(r_t - d_{p1p3}, r_t - d_{p1p3}), & if \, r_r - d_{p1p3} > 0 \\ 0 & if \, r_r - d_{p1p3} < 0 \end{cases} \quad (11)$$

Considering tool runout effect, Eq. (11) could be induced as follows.

The tool edge with constant lead can be expressed in the $X_T Y_T Z_T\text{-}O_T$ coordinates as:

Fig. 6 Calculation principle of UCT with considering runout effect ($r_t = 0.25$ mm, $f_t = 0.006$ mm, $y_{out} = 0.01$ mm)
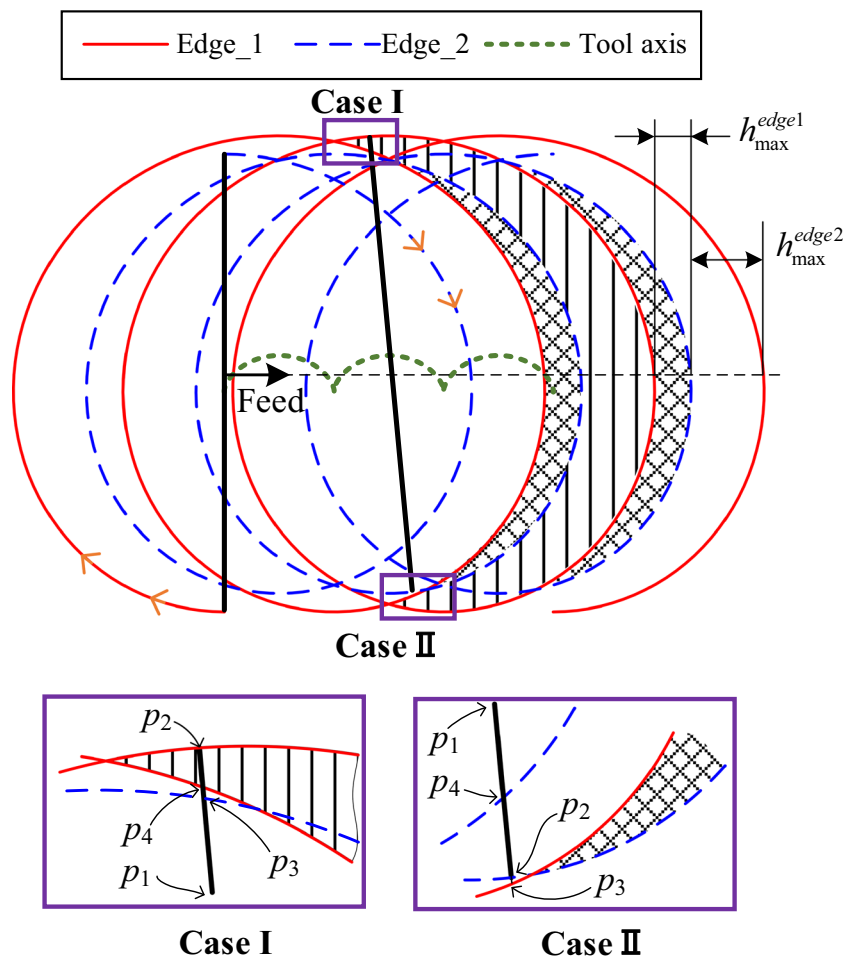
$$r_{edge\_1}^T(l_{tz}) = \begin{bmatrix} x_{edge\_1}^T \\ y_{edge\_1}^T \\ z_{edge\_1}^T \end{bmatrix} = \begin{bmatrix} -r_t\sin(2\pi l_{tz}/P + 2\pi(i-1)/N) \\ r_t\cos(2\pi l_{tz}/P + 2\pi(i-l)/N) \\ l_{tz} \end{bmatrix} \quad (12)$$

where P is lead, N is the number of edges, l_{tz} is the distance between the point on the edge, and the $X_T Y_T$-O_T plane, as shown in Fig. 1(b).

Due to the tool runout, the tool axis (Z_T-axis) does not coincide with the machine tool spindle (Z_S-axis). And the transformation matrix from the tool coordinates ($X_T Y_T Z_T$-O_T) to the spindle coordinates ($X_S Y_S Z_S$-O_S) can be deduced as:

$$\mathbf{M\_f_t} = \begin{bmatrix} 1 & 0 & 0 & 0 \\ 0 & 1 & 0 & y_{out} \\ 0 & 0 & 1 & 0 \\ 0 & 0 & 0 & 1 \end{bmatrix} \quad (13)$$

During the milling process, the tool rotates around the spindle, and the rotational transfer matrix can be expressed as:

$$\mathbf{M\_rot} = \begin{bmatrix} \cos(-\phi) & -\sin(-\phi) & 0 & 0 \\ \sin(-\phi) & \cos(-\phi) & 0 & 0 \\ 0 & 0 & 1 & 0 \\ 0 & 0 & 0 & 1 \end{bmatrix} \quad (14)$$

where φ is the tool rotation angle around the spindle (Z_S-axis).

The tool moves along the X_W-axis with the speed f_t, and the transfer matrix can be written as:

$$\mathbf{M\_f_t} = \begin{bmatrix} 1 & 0 & 0 & f_t N\phi/2\pi \\ 0 & 1 & 0 & 0 \\ 0 & 0 & 1 & 0 \\ 0 & 0 & 0 & 1 \end{bmatrix} \quad (15)$$

Then, the sweep surface generated by the tool edge during the milling process can be deduced in the workpiece coordinates as:

$$\mathbf{r}_{si}^W(l_{tx}, \phi) = \begin{bmatrix} x_{si}^W \\ y_{si}^W \\ z_{si}^W \\ 1 \end{bmatrix} = \mathbf{M\_f_t} \cdot \mathbf{M\_rot} \cdot \mathbf{M\_runout} \cdot \begin{bmatrix} x_{edge\_i}^T \\ y_{edge\_i}^T \\ z_{edge\_i} \\ 1 \end{bmatrix} \quad (16)$$

The point $Q = (x_Q^W, y_Q^W, z_Q^W)$ on the cutting edge can be calculated in the workpiece coordinates according to Eq. (16). Three conditions have to be checked to decide whether the point Q is involved in the cutting process: (1) the point should in the range of cutting depth ($z_Q^W < a_p$, in Fig. 7); (2) the point should in the range of cutting width ($y_Q^W < a_e - r_t$, in Figs. 7 and 3 the point should in the range of the previous cutting edge trajectory($dh_j > 0$, in Fig. 6).

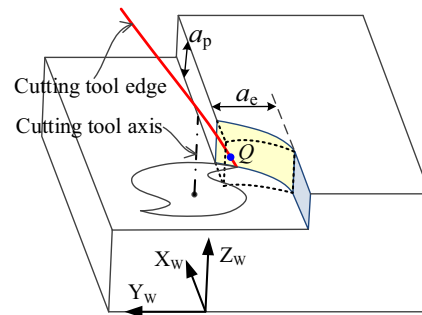Then, the micro-milling force with tool runout and wear effect based on the SAG method can be modeled as follows.

Fig. 7 Illustration of cutting edges involved in the milling process

Step 1: the resultant and mean cutting forces in different tool wear states are calculated by micro-slot milling experiments.

Step 2: with the known milling parameters a_p, a_e, f_t and n, the runout parameter y_{out} is calculated by using Eq. (9) with the resultant forces, which are measured with the fresh tool.

Step 3: the force model with considering runout parameter y_{out} is established with unknown variables K_{tc}, K_{rc}, K_{tc}^{wear} and K_{rc}^{wear}. Accordingly, these variables are calibrated by substituting the mean forces in different tool wear states into Eq. (10).

Thus, the runout parameter y_{out} and the force coefficients K_{tc} and K_{rc} are calibrated with the known a_p, a_e, f_t, n, and experiments and the force model are established.

3 Experimental validation

3.1 Experimental setup

In order to verify the established model, micro-milling experiments were designed by Taguchi method, as provided in Table 1. The Taguchi L9 array with three factors and three

Table 1 Taguchi design of micro-milling

Number	Milling parameters				Other conditions
	n/rpm	v_c/m min^{-1}	a_p/ μm	f_t/ μm·tooth^{-1}	
No. 1	18,000	28	60	2	Slot milling
No. 2	18,000	28	80	4	Dry milling
No. 3	18,000	28	100	6	Solid carbide end mill
No. 4	24,000	38	80	6	Tool diameter: 0.5 mm
No. 5	30,000	47	60	6	Tool helical angle: 30 degrees
No. 6	24,000	38	60	4	Workpiece material: AISI4340
No. 7	24,000	38	100	2	
No. 8	30,000	47	80	2	
No. 9	30,000	47	100	4	

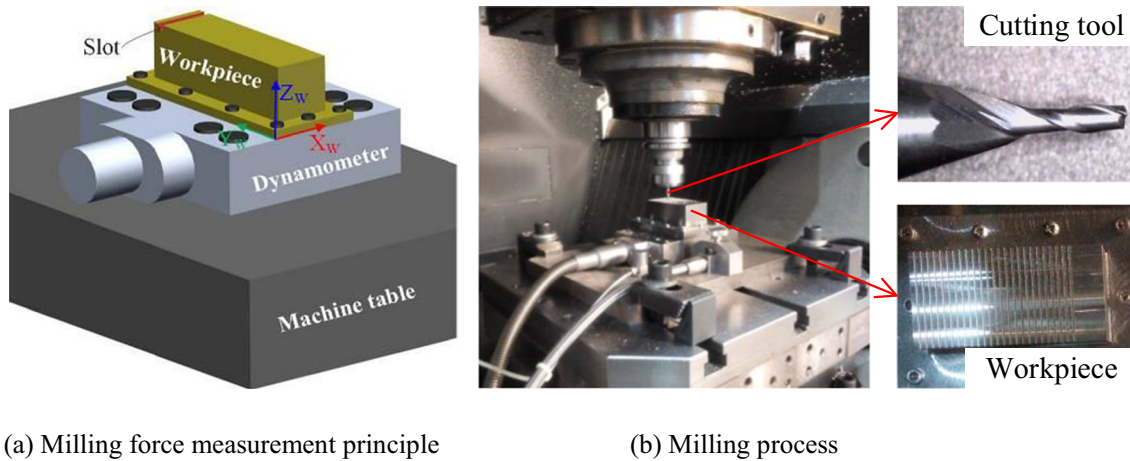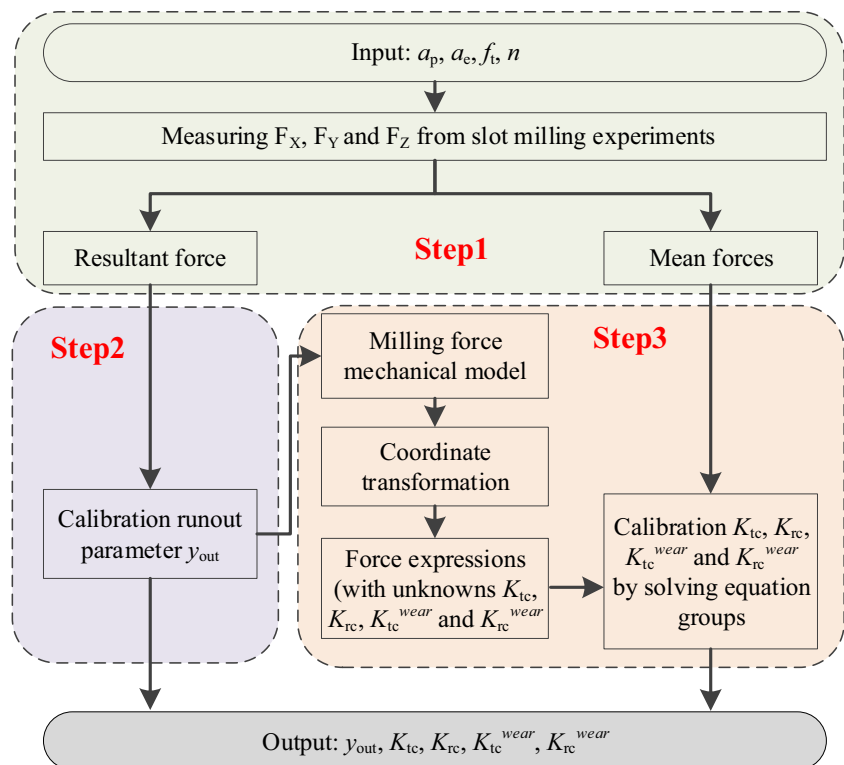(a) Milling force measurement principle   (b) Milling process

Fig. 8 Micro-milling experiment. **a** Milling force measurement principle. **b** Milling process

levels was used. The factors included cutting speed, cutting depth and feed per tooth. During the experiment, cutting forces and tool wears were measured. The experiments were carried out by the high-speed machining center MIKRON HSM600U, as shown in Fig. 8. The cutting force was measured by the Kistler 9119AA2 dynamometer, and the sampling frequency was 24 KHz. The tool wear was measured per cutting length with 60 mm. With the calculated runout parameter y_{out}, the force coefficients could be calibrated by using the mean force method. The overall approach of milling force coefficients determination is shown in Fig. 9.

3.2 Validations

3.2.1 Validation of the developed model with considering tool runout

Based on the measured milling forces, the runout parameter and the force coefficients of the model were calibrated with the method introduced in Fig. 9. As a comparison, they were also calculated by the traditional method without considering runout. The results were listed in Table 2.

Fig. 9 Calibration processes of milling force coefficients with considering runout

Table 2 Results of milling force coefficients with or without considering runout

Number	With considering runout			Without considering runout (traditional method)	
	y_{out} (μm)	K_{tc}	K_{rc}	K_{tc}' (Relative variation/%)	K_{rc}' (Relative variation/%)
No. 1	0.333	18,890	12,057	18,818 (0.4)	12,156 (0.8)
No. 2	0.182	15,394	10,235	15,333 (0.4)	10,306 (0.7)
No. 3	0.020	9493	7301	9489 (0.04)	7305 (0.05)
No. 4	0.600	8117	5851	8065 (0.6)	5908 (1.0)
No. 5	0.176	10,464	6406	10,439 (0.2)	6439 (0.5)
No. 6	0.500	12,845	9470	12,785 (0.5)	9541 (0.7)
No. 7	0.139	15,946	12,935	15,841 (0.7)	13,030 (0.7)
No. 8	0.100	17,994	14,242	17,918 (0.4)	14,318 (0.5)
No. 9	0.050	16,343	11,983	16,320 (0.1)	12,007 (0.2)

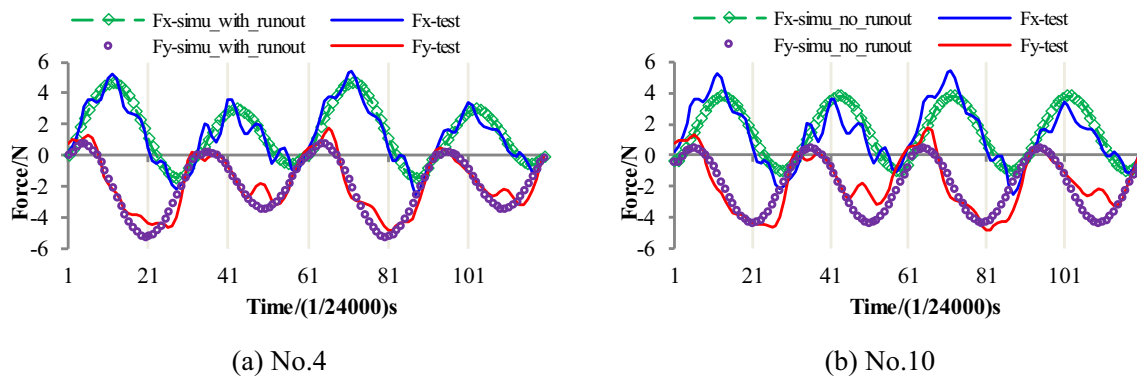(a) No.4   (b) No.10

Fig. 10 Results of simulations and experiments

Then, substituting y_{out}, K_{tc}, and K_{rc} into Eq.(2) and Eq.(11), the milling force model was established by using the UCT calculation method introduced in section 2.2 and the criteria of cutting edges involved in the cutting process discussed in section 2.3. Accordingly, nine time domain waveforms of the milling forces in one revolution. Figure 10(a) presented the No. 4 test as an example. As a comparison, an auxiliary simulation without considering runout was conducted, which corresponded to No. 4 test and denoted as No. 10, as shown in Fig. 10(b).

Furthermore, the standard deviations and errors of mean forces between the simulations and the experiments were calculated in Fig. 11. The results of No. 1 to No. 9 showed that errors of standard deviations were less than 1.0 Newton (except No. 9) and errors of mean forces were under 10%. Thus, the established model was proved to be reliable.

The error of mean forces between the simulations and the tests was calculated by (Fs-Ft)/Ft, where "Fs" was the simulation result and "Ft" was the test results. It showed that all the mean errors were negative. It was because the plow force was

Fig. 11 Error analysis of the simulations and experiments. **a** Stand deviation analysis. **b** Mean force error analysis

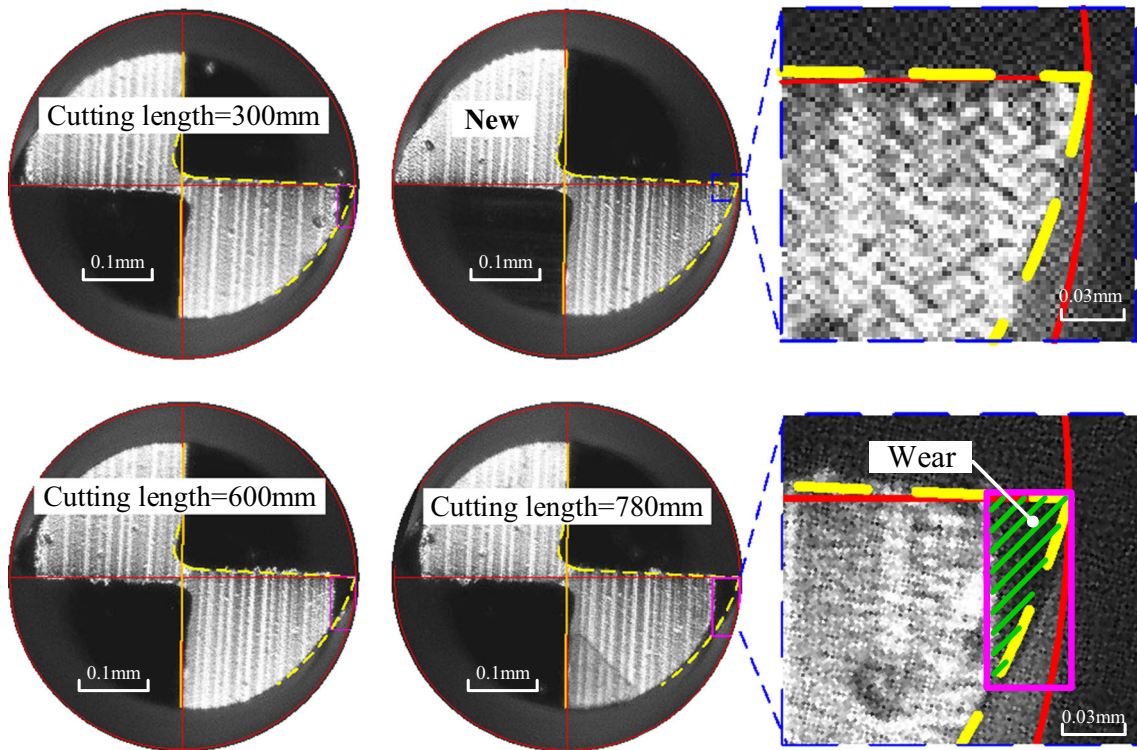(a) Stand deviation analysis   (b) Mean force error analysis
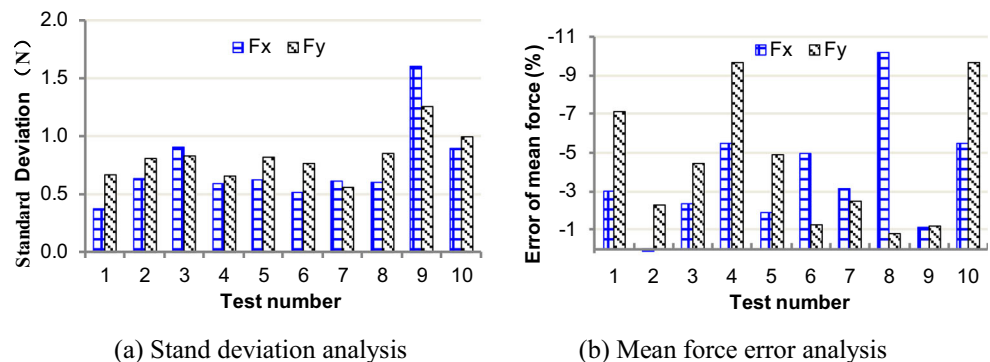
Fig. 12 Tool wear definition and increasing processes during the micro-milling experiments of No. 3

neglected in the established simulation model which leads to the simulation results that were smaller than the test.

Besides, comparing No. 4 with No. 10, it showed that with considering runout, the standard deviations and the error of mean forces between the simulations and the experiments were decreased (Fig. 11), and the simulation waveforms got better coincidence with the experiments (Fig. 10). It was because that the different UCTs of each edge induced by runout modified the tradition modal. Therefore, the different forces corresponding to different edges could be revealed, which was more coincide with the practice. However, Table 2 showed that the relative variation of force coefficients was under 1%, which means that the force coefficients change little with or without considering

runout. Thus, it could be concluded that considering runout in the micro-milling force model will improve its accuracy, even if it had little impact on the force coefficients.

3.2.2 Validation of the developed model with considering tool wear

The micro-milling tool wear was measured in the end faces and expressed by the wear area. Figure 12 showed the tool wear processes during the micro-milling experiments of No. 3 (in Table 1). Considering that the two edges had different wear because of runout, the edge with larger wear was evaluated.
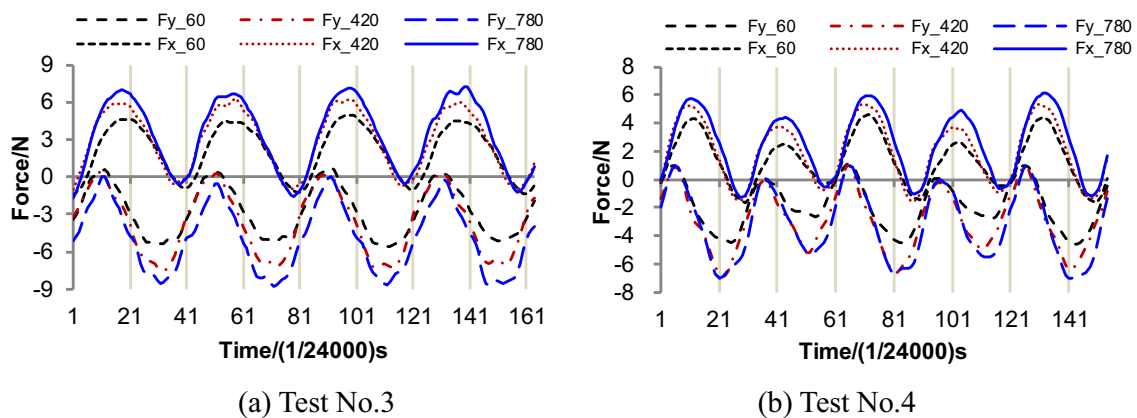

Fig. 13 Cutting force signals with 60,420 and 780 mm cutting length

With the same method, the other eight tools used in Table 1 were measured.

According to Table 2, the No. 3 test had a little runout and No. 4 had a larger runout. Thus, these typical two tests were selected to validate the force model considering tool wear. The time-domain waveforms of the two tests with cutting lengths of 60, 420, and 780 mm were presented in Fig. 13. It showed that the shape of the force waveforms changed little with the tool wear, even if the force value was increased. So, the force model considering tool wear had the similar expression with Eq. (2), just as introduced in Eq. (10).

3.3 Discussions
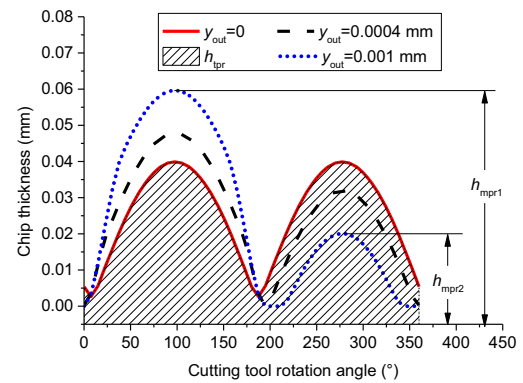
3.3.1 Influence of tool runout on the model

According to Eq. (11), the influence of runout on the UCT was provided in Fig. 14. Figure 14(a) presented the instantaneous chip thickness of the tool when the runout was 0, 0.4 μm, and 1 μm. The total chip thickness (h_{tpr}) was calculated in a period of rotation. The maximum chip thickness for the two edges is denoted as h_{mpr1} and h_{mpr2}, respectively.

Figure 14(b) illustrated the influence of runout on the h_{tpr}. It showed that when the runout increased by 400% (i.e., from 0.2 to 1 μm), the h_{tpr} was only a 0.3% increase. In conclusion, the h_{tpr} changed little with the increase of runout. It was the same for the mean chip thickness because it was only related to the h_{tpr}. As the force coefficients were calibrated by using the mean force method, namely the coefficient is the ratio of mean force to the mean chip thickness, the force coefficients changed little with runout increased, which explained the result that listed in Table 2.

Figure 14(c) showed the influence of runout on the maximum chip thickness of different cutting edges. It indicated that when the runout increased by 400% (i.e., from 0.2 μm to 1 μm), the difference between the maximum chip thickness of two edges (i.e., h_{mpr1}-h_{mpr2}) was about 478% increase (calculated as 100% × (0.0579–0.0201)/(0.0439–0.0360)). In conclusion, the h_{mpr1}-h_{mpr2} changed greatly with the increase of runout, which means that different cutting edges would suffer unequal maximum cutting forces with tool runout. Therefore, it was reasonable to calibrated tool runout with the maximum cutting forces of different cutting edges, and Eq. (9) was supported.

### 3.3.2 Influence of tool wear on the model

The tool wear and its influence on milling forces of the 9 tests were provided in Fig. 15. The tool wear was measured in the end faces and expressed by the wear area (Fig. 15(a)) rather than the ISO standards ISO8688-1 and ISO8688-2 because the later cannot meet the requirement for micromilling. Accordingly, the tool wears were found to be

(a) Instantaneous UCT of per cutting tool rotation
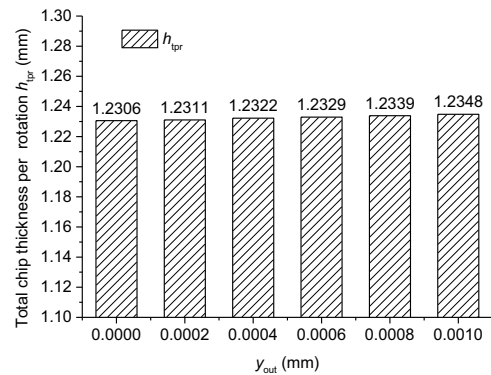
(b) Changes of total chip thickness per revolution
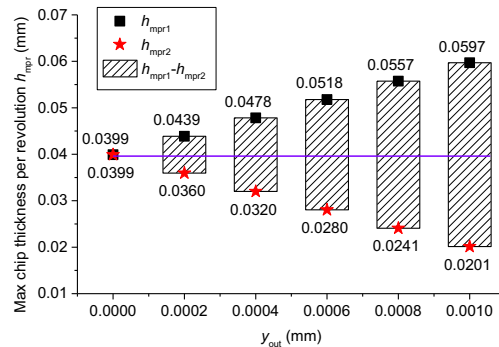
(c) Difference between the maximum chip thicknesses of two edges

Fig. 14 Influence of runout on the UCT ($r_t = 0.25$ mm, $f_t = 0.004$ mm, $a_e = 0.5$ mm, $a_p = 0.1$ mm). **a** Instantaneous UCT of per cutting tool rotation. **b** Changes of total chip thickness per revolution. **c** Difference between the maximum chip thicknesses of two edges

approximately proportional to the cutting length, which was different from the traditional milling, as provided in Fig. 15(a).

Considering that the maximum forces were more essential than the mean forces for the milling processes, the quantitative relationship between the maximum force and tool wear was investigated. The maximum forces of the nine tests at different wear stages were plotted in Fig. 15(b) and (c). They showed that the maximum forces in the Fx and Fy directions also exhibit an approximately linear increase with cutting length. According to Fig.15(a), it could be concluded that the

Fig. 15 Tool wear influence on milling force. **a** Tool wear value. **b** Maximum of Fx changes with tool wear. **c** Maximum of Fy changes with tool wear. **d** Proportions of the "maximum milling forces-cutting length" slope and the "tool wear- cutting length" slope
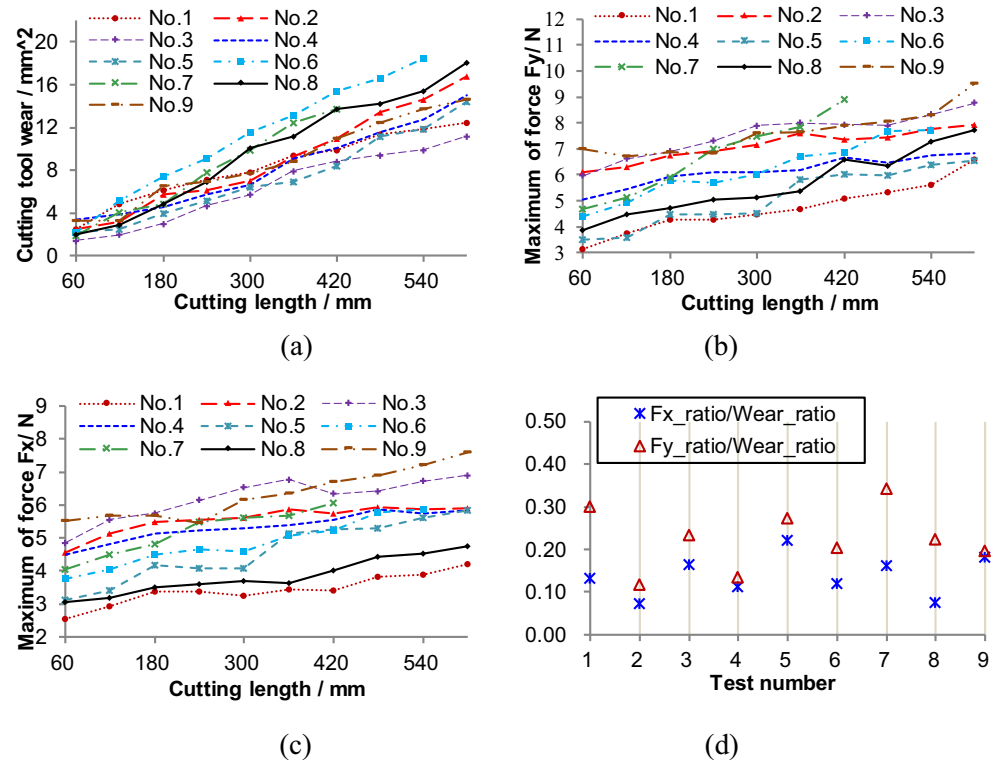
relationship between the forces and tool wear could be converted to the relationship between the two slopes, just as provided in Fig.15(d). The proportion of the two slops for a test was denoted as "Fx_ratio / Wear_ratio" and "Fy_ratio / Wear_ratio" and the Wear_ratio, Fx_ratio and Fy_ratio were calculated from Fig. 1(a), Figs. 1 (b) and (c), respectively. The results indicated that the tool wear had a larger impact on the coefficients of Fx than that of Fy. Namely, the tool wear had a larger impact on the forces in the feed direction.

4 Conclusions

Modeling micro-milling force with considering tool runout and wear was crucial to enhance the understanding of the micro-milling mechanics as well as to optimize the process. While the tool runout parameters were difficult to be calibrated due to their small scale, and the impact of tool wear on the milling force was hard to be identified. By using the SAG method, a new force model with considering tool runout and wear was proposed in the paper. The tool runout could be rapidly identified by the measured milling forces, and the force model with considering tool wear can be uniformly expressed as an accrementition of coefficients of a fresh tool. The results had shown that the error of standard deviations between the simulations and the experiments was less than 1.0 Newton and the error of mean forces was under 10%, which means that the established model with considering tool

runout could achieve high accuracy. Furthermore, the tool wear has greater impact on the forces in the feed direction than that of the direction perpendicular to the feed. The tool wear, measured in the end faces and expressed by the wear area, was approximately proportional to the cutting length in micro-milling processes, which is different from the traditional milling processes.

References

1. Zhang X, Yu T, Wang W, Zhao J (2019) Improved analytical prediction of burr formation in micro end milling. Int J Mech Sci 151: 461–470. https://doi.org/10.1016/j.ijmecsci.2018.12.005

2. Davim JP (2014) Modern mechanical engineering. Materials Forming, Machining and Tribology. https://doi.org/10.1007/978-3-642-45176-8

3. Mian AJ, Driver N, Mativenga PT (2011) Estimation of minimum chip thickness in micro-milling using acoustic emission. 225 (9): 1535-1551. https://doi.org/10.1177/0954405411404801

4. Kang IS, Kim JS, Kim JH, Kang MC, Seo YW (2007) A mechanistic model of cutting force in the micro end milling process. J Mater Process Technol 187-188:250–255. https://doi.org/10.1016/j.jmatprotec.2006.11.155

5. Afazov SM, Ratchev SM, Segal J (2010) Modelling and simulation of micro-milling cutting forces. J Mater Process Technol 210(15): 2154–2162. https://doi.org/10.1016/j.jmatprotec.2010.07.033

6. Afazov SM, Zdebski D, Ratchev SM, Segal J, Liu S (2013) Effects of micro-milling conditions on the cutting forces and process stability. J Mater Process Technol 213(5):671–684. https://doi.org/10.1016/j.jmatprotec.2012.12.001

7. Davoudinejad A, Tosello G, Parenti P, Annoni M (2017) 3D finite element simulation of micro end-milling by considering the effect of tool run-out. Micromachines-Basel 8(6). https://doi.org/10.3390/mi8060187

8. Chen N, Li L, Wu J, Qian J, He N, Reynaerts D (2019) Research on the ploughing force in micro milling of soft-brittle crystals. Int J Mech Sci 155:315–322. https://doi.org/10.1016/j.ijmecsci.2019.03.004

9. Kang Y-H, Zheng CM (2012) Fourier analysis for micro-end-milling mechanics. Int J Mech Sci 65(1):105–114. https://doi.org/10.1016/j.ijmecsci.2012.09.008

10. Wojciechowski S, Mrozek K (2017) Mechanical and technological aspects of micro ball end milling with various tool inclinations. Int J Mech Sci 134:424–435. https://doi.org/10.1016/j.ijmecsci.2017.10.032

11. Sahoo P, Pratap T, Patra K (2019) A hybrid modelling approach towards prediction of cutting forces in micro end milling of Ti-6Al-4V titanium alloy. Int J Mech Sci 150:495–509. https://doi.org/10.1016/j.ijmecsci.2018.10.032

12. Arrazola PJ, Özel T, Umbrello D, Davies M, Jawahir IS (2013) Recent advances in modelling of metal machining processes. CIRP Ann 62(2):695–718. https://doi.org/10.1016/j.cirp.2013.05.006

13. Jing X, Tian Y, Yuan Y, Wang F (2017) A runout measuring method using modeling and simulation cutting force in micro end-milling. Int J Adv Manuf Technol 91(9–12):4191–4201. https://doi.org/10.1007/s00170-017-0076-9

14. Matsumura T, Tamura S (2017) Cutting force model in milling with cutter runout. Procedia CIRP 58:566–571. https://doi.org/10.1016/j.procir.2017.03.268

15. Dadgari A, Huo D, Swailes D (2018) Investigation on tool wear and tool life prediction in micro-milling of Ti-6Al-4V. Nanotech Precis Eng 1(4):218–225. https://doi.org/10.1016/j.npe.2018.12.005

16. Alhadeff LL, Marshall MB, Curtis DT, Slatter T (2019) Protocol for tool wear measurement in micro-milling. Wear 420-421:54–67. https://doi.org/10.1016/j.wear.2018.11.018

17. Li Z-L, Zhu L-M (2014) Envelope surface modeling and tool path optimization for five-axis flank milling considering cutter Runout. J Manuf Sci E-T ASME 136(4):041021–041029. https://doi.org/10.1115/1.4027415

18. Li Z-L, Niu J-B, Wang X-Z, Zhu L-M (2015) Mechanistic modeling of five-axis machining with a general end mill considering cutter runout. Int J Mach Tool Manu 96:67–79. https://doi.org/10.1016/j.ijmachtools.2015.06.006

19. Zhu Z, Yan R, Peng F, Duan X, Zhou L, Song K, Guo C (2016) Parametric chip thickness model based cutting forces estimation considering cutter runout of five-axis general end milling. Int J Mach Tool Manu 101:35–51. https://doi.org/10.1016/j.ijmachtools.2015.11.001

20. Zhang X, Yu T, Wang W (2018) Prediction of cutting forces and instantaneous tool deflection in micro end milling by considering tool run-out. Int J Mech Sci 136:124–133. https://doi.org/10.1016/j.ijmecsci.2017.12.019

21. Yun W-S, Cho D-W (2000) An improved method for the determination of 3D cutting force coefficients and runout parameters in end milling. Int J Adv Manuf Technol 16(12):851–858. https://doi.org/10.1007/s001700070001

22. Hoon Ko J, Cho D-W (2005) 3D ball-end milling force model using instantaneous cutting force coefficients. J Manuf Sci E-T ASME 127(1):1–12. https://doi.org/10.1115/1.1826077

23. Li K, Zhu K, Mei T (2016) A generic instantaneous undeformed chip thickness model for the cutting force modeling in micromilling. Int J Mach Tool Manu 105:23–31. https://doi.org/10.1016/j.ijmachtools.2016.03.002

24. Wan M, Zhang W-H, Dang J-W, Yang Y (2009) New procedures for calibration of instantaneous cutting force coefficients and cutter runout parameters in peripheral milling. Int J Mach Tool Manu 49(14):1144–1151. https://doi.org/10.1016/j.ijmachtools.2009.08.005

25. Zhang X, Zhang J, Pang B, Zhao W (2016) An accurate prediction method of cutting forces in 5-axis flank milling of sculptured surface. Int J Mach Tool Manu 104:26–36. https://doi.org/10.1016/j.ijmachtools.2015.12.003

26. Guo Q, Sun Y, Guo D, Zhang C (2012) New mathematical method for the determination of cutter runout parameters in flat-end milling. Chin J Mech Eng 25(5):947–952. https://doi.org/10.3901/cjme.2012.05.947

27. Zhang X, Pan X, Wang G, Zhou D (2018) Tool runout and single-edge cutting in micro-milling. Int J Adv Manuf Technol 96(1):821–832. https://doi.org/10.1007/s00170-018-1620-y

28. Attanasio A (2017) Tool run-out measurement in micro milling. Micromachines (Basel) 8(7). https://doi.org/10.3390/mi8070221

29. Tansel IN, Arkan TT, Bao WY, Mahendrakar N, Shisler B, Smith D, McCool M (2000) Tool wear estimation in micro-machining.: part II: neural-network-based periodic inspector for non-metals. Int J Mach Tool Manu 40(4):609–620. https://doi.org/10.1016/S0890-6955(99)00074-7

30. Robinson GM, Jackson MJ, Whitfield MD (2007) A review of machining theory and tool wear with a view to developing micro and nano machining processes. J Mater Sci 42(6):2002–2015. https://doi.org/10.1007/s10853-006-0171-z

31. Malekian M, Park SS, Jun MBG (2009) Tool wear monitoring of micro-milling operations. J Mater Process Technol 209(10):4903–4914. https://doi.org/10.1016/j.jmatprotec.2009.01.013

32. Abdelrahman Elkaseer AM, Dimov SS, Popov KB, Minev RM (2014) Tool wear in micro-endmilling: material microstructure effects, modeling, and experimental validation. J Micro Nano Manuf 2(4):044502–044510. https://doi.org/10.1115/1.4028077

33. Bao WY, Tansel IN (2000) Modeling micro-end-milling operations. Part III: influence of tool wear. Int J Mach Tool Manu 40(15):2193–2211. https://doi.org/10.1016/S0890-6955(00)00056-0

34. Oliaei SNB, Karpat Y (2016) Influence of tool wear on machining forces and tool deflections during micro milling. Int J Adv Manuf Technol 84(9):1963–1980. https://doi.org/10.1007/s00170-015-7744-4

35. Lu X, Wang F, Jia Z, Si L, Zhang C, Liang SY (2017) A modified analytical cutting force prediction model under the tool flank wear effect in micro-milling nickel-based superalloy. Int J Adv Manuf Technol 91(9–12):3709–3716. https://doi.org/10.1007/s00170-017-0001-2

36. Thepsonthi T, Özel T (2015) 3-D finite element process simulation of micro-end milling Ti-6Al-4V titanium alloy: experimental validations on chip flow and tool wear. J Mater Process Technol 221:128–145. https://doi.org/10.1016/j.jmatprotec.2015.02.019

37. Jaffery SHI, Khan M, Ali L, Mativenga PT (2016) Statistical analysis of process parameters in micromachining of Ti-6Al-4V alloy 230 (6):1017–1034. https://doi.org/10.1177/0954405414564409

38. Yoon HS, Ehmann KF (2016) Dynamics and stability of micro-cutting operations. Int J Mech Sci 115-116:81–92. https://doi.org/10.1016/j.ijmecsci.2016.06.009

39. Germain D, Fromentin G, Poulachon G, Bissey-Breton S (2013) From large-scale to micromachining: a review of force prediction models. J Manuf Process 15(3):389–401. https://doi.org/10.1016/j.jmapro.2013.02.006